THE UNIVERSITY of EDINBURGH

Edinburgh Research Explorer

Carbon Dioxide-Dependent Regulation of NF-B Family Members RelB and P100 Gives Molecular Insight Into CO2-dependent Immune Regulation

Citation for published version:
Keogh, CE, Scholz, CC, Rodriguez, J, Selfridge, AC, Von Kriegsheim, A & Cummins, EP 2017, 'Carbon Dioxide-Dependent Regulation of NF-B Family Members RelB and P100 Gives Molecular Insight Into CO2-dependent Immune Regulation', *Journal of Biological Chemistry*, pp. jbc.M116.755090. https://doi.org/10.1074/jbc.M116.755090

Digital Object Identifier (DOI):
10.1074/jbc.M116.755090

Link:
Link to publication record in Edinburgh Research Explorer

Document Version:
Peer reviewed version

Published In:
Journal of Biological Chemistry

General rights
Copyright for the publications made accessible via the Edinburgh Research Explorer is retained by the author(s) and / or other copyright owners and it is a condition of accessing these publications that users recognise and abide by the legal requirements associated with these rights.

Take down policy
The University of Edinburgh has made every reasonable effort to ensure that Edinburgh Research Explorer content complies with UK legislation. If you believe that the public display of this file breaches copyright please contact openaccess@ed.ac.uk providing details, and we will remove access to the work immediately and investigate your claim.

OPEN ACCESS

Download date: 04. May. 2023

Carbon dioxide-dependent regulation of NF-κB family members RelB and p100 gives molecular insight into CO_2 – dependent immune regulation.

Ciara E. Keogh[1], Carsten C. Scholz [2,4], Javier Rodriguez[2,3], Andrew C. Selfridge[1], Alexander von Kriegsheim[2,3], Eoin P. Cummins[1]

[1]School of Medicine & Conway Institute University College Dublin, [2]Systems Biology Ireland, [3] Edinburgh Cancer Research Centre, [4]Institute of Physiology, University of Zurich

ABSTRACT

CO_2 is a physiological gas normally produced in the body during aerobic respiration. Hypercapnia (elevated blood pCO_2 > ≈ 50mmHg) is a feature of several lung pathologies e.g. chronic obstructive pulmonary disease (COPD). Hypercapnia is associated with increased susceptibility to bacterial infections and suppression of inflammatory signaling. The NF-κB pathway has been implicated in these effects, however, the molecular mechanisms underpinning cellular sensitivity of the NF-κB pathway to CO_2 is not fully elucidated. Here we identify several novel CO_2-dependent changes in the NF-κB pathway. NF-κB family members p100 and RelB translocate to the nucleus in response to CO_2. A cohort of RelB protein-protein interactions (e.g. with Raf-1 and IκBα) are altered by CO_2 exposure, while others are maintained (e.g. with p100). RelB is processed by CO_2 in a manner dependent on a key C-terminal domain located in its transactivation domain. Loss of the RelB transactivation domain alters NF-κB -dependent transcriptional activity and loss of p100 alters sensitivity of RelB to CO_2. Thus, we provide molecular insight into the CO_2-sensitivity of the NF-κB pathway and implicate altered RelB/p100-dependent signaling in the CO_2-dependent regulation of inflammatory signaling.

INTRODUCTION

Oxygen (O_2) and carbon dioxide (CO_2) are the substrate and product of aerobic respiration respectively. Atmospheric CO_2 levels have recently exceeded 400ppm (0.04%) with the highest ever daily average CO_2 recorded at Mauna Loa Observatory in April 2016 (409.44ppm) (www.co2.earth). While the levels of this greenhouse gas are rising, the levels in the atmosphere are still much lower than that experienced within respiring organisms. CO_2 is produced as a consequence of aerobic respiration during the pre-Kreb's and Kreb's cycle reactions. Thus, in normocapnia the normal pCO_2 in the human circulation is approximately 40mmHg. Because, the main mechanism through which CO_2 is removed from the body is via exhalation, the circulating pCO_2 is closely related to lung function and ventilation. Hyperventilation can result in lower than normal levels of CO_2 (hypocapnia) and hypoventilation and/or chronic lung diseases such as chronic obstructive pulmonary disease and cystic fibrosis result in elevated levels of CO_2 (hypercapnia)(1). In patients the degree of hypercapnia can be profound with arterial pCO_2 values in excess of 100mmHg recorded in exacerbated COPD (2). Hypocapnia is associated with a worse outcome in COPD (3) and worsens cerebral ischemia (4). Interestingly, hypercapnia is also associated with a worse outcome in COPD (3) with additional deleterious consequences reported in terms of muscle dysfunction (5) and immunosuppression (6). This evidence indicates that carbon dioxide is not merely a waste product of metabolism and that like oxygen it can elicit a specific repertoire of transcriptional events in a dose dependent fashion (1,7). In particular, genes associated with inflammation, immunity and metabolism appear to be CO_2 sensitive and that sensitivity of these cohorts of genes to CO_2 is evolutionarily conserved (8-10). The mechanisms however, are not well characterized. We and others have previously demonstrated sensitivity of the NF-κB pathway to CO_2 (11-16) and elevated CO_2 is associated with suppression of pro-inflammatory cytokines in a number of different settings (11,12,17). The current state of the art is that hypercapnia may be damaging in the context of infection (6,18) due to immunosuppression. Conversely, hypercapnia may be of benefit in the context of destructive inflammation (19,20) due to suppression of inflammatory signaling (1,21). Given the importance of the NF-κB pathway in the regulation of immune and inflammatory signaling, we hypothesise that CO_2-dependent alterations in NF-κB is important in determining inflammatory signaling over a range of pCO_2 values from hypocapnia to normocapnia to hypercapnia. Our previous work has implicated members of the non-

canonical NF-κB pathway (IKKα and RelB) as being particularly sensitive to changes in CO_2 in the basal (unstimulated) state (11,12). The current study gives molecular insight into CO_2-dependent modulation of the NF-κB transcription factor RelB.

NF-κB is a family of five transcription factors p50, p65, p52, RelB and cRel. Of these, p65 is the transcriptionally active component of the canonical p65-p50 heterodimer that is activated downstream of the hetero-trimeric IKKα,β,γ complex (22). RelB on the other hand is the transcriptionally active component of the non-canonical RelB-p52 heterodimer that is activated downstream of an IKKα homodimer complex (23). Canonical signaling is associated with the regulation of classical pro-inflammatory gene activation e.g. TNFα, IL-6 and IL-1 (mainly via p65/p50 heterodimers) while non-canonical NF-κB signaling is associated with regulation of genes involved in lymphogenesis development (24,25) (mainly via RelB/p52 heterodimers). Both canonical and non-canonical NF-κB family members demonstrate sensitivity to CO_2 in the stimulated state (11) however, non-canonical family members IKKα and RelB appear much more sensitive to CO_2 in the basal (non-ligand stimulated) state (12).

RelB is has been dubbed 'an outlier in leukocyte biology' (23) and is relatively less well characterised than p65. RelB uniquely possesses an N-terminal leucine zipper domain which affects the ability of RelB to activate transcription of target genes (26), furthermore it is postulated that RelB can activate a more diverse array of NF-κB consensus binding sequences than other family members (27). The RelB c-terminal contains a TAD which is conserved amongst RelA, RelB and c-Rel (25). Pathways regulated by RelB include those involved in **(i)** immune development and signaling, (24,28) **(ii)** response to xenobiotics (29), **(iii)** chromatin remodeling e.g. RelB can associate with the ATP-dependent SWI/SNF nucleosome-remodelling complex (30) **(iv)** circadian rhythms (31) and **(v)** cellular metabolism (23). Thus, RelB can modulate an array of cellular responses. The molecular mechanisms underpinning these effects are not yet fully appreciated. Taken together, it is clear that RelB differs significantly from other NF-κB family members in terms of structure, regulation and target gene expression. Indeed, the relative contribution of both RelA and RelB to Lymphotoxin- induced gene expression reveals both overlapping and subunit-specific target genes (32).

RelB is a labile protein subject to significant post-translational modification. Elegant biochemical studies have illustrated that RelB is a target for phosphorylation (33,34), ubiquitination (35), sumoylation (36) , signal-induced degradation and cleavage (33,37). These modifications regulate RelB function as well as protein-protein interactions. The protein-protein interaction between RelB and p100 is particularly important for their respective functions (34). p100 acts as an inhibitor of RelB as well as facilitating a 'co-operative stabilizing state' between the two proteins (23). p100 in addition to stabilizing and inhibiting RelB has been shown to inhibit canonical NF-κB-dependent transcription via sequestration of RelA-p50 dimers (38). Recent work has highlighted the association of RelB (along with other NF-κB subunits) with p100 as part of a high-molecular- weight repressive 'kappaBsome' (39,40).

Finally, a recent study identified RelB mRNA expression as being associated with acid-base and cardiovascular features in patients with exacerbated COPD (41), suggesting a functional regulation of this NF-κB family member in a serious disease where hypercapnia is prevalent. The detailed mechanisms underpinning the CO_2-dependent modulation of p100 and RelB along with the downstream consequences for NF-κB-dependent signaling beyond this have not yet been elucidated and are the focus of this study.

RESULTS

Elevated CO_2 causes a cellular re-organisation of the NF-κB family members RelB and p100.

We have previously reported that exposure of cells to elevated CO_2 induces RelB nuclear localisation and cleavage in a number of cell types. The mechanisms underpinning this

CO_2-dependent modulation of immune signaling are not fully understood and is a focus of this study. Here we demonstrate in mouse embryonic fibroblasts (MEF) a CO_2-dependent nuclear localization and cleavage of RelB that is evident over a range of CO_2 conditions (.03%, 5% and 10% CO_2) **(Fig.1A & D).** We observed a very similar pattern in lung epithelial A549 cells (**Fig. S1A-C**). This CO_2-dose- dependent regulation of NF-κB from hypocapnia, to normocapnia to hypercapnia highlights the importance of considering the impact of microenvironmental CO_2 concentrations in a range of conditions.

Given that RelB functionally interacts with p100 within the non-canonical NF-κB pathway, we next investigated whether p100 also demonstrated sensitivity to CO_2. Interestingly, we observed sensitivity of the p100 -sub unit to CO_2. This is the first time that p100-sensitivity to CO_2 has been reported to our knowledge. p100 markedly translocates to the nucleus following exposure to 5% CO_2 and 10% CO_2 **(Fig.1A & E.)**. We observed a very similar pattern in lung epithelial A549 cells **(Fig.S1A, D & E)** with a more marked difference observed between 5% and 10% CO_2 in these cells. Thus, in the basal (unstimulated state) members of the non-canonical NF-κB family undergo cellular modification and re-organisation by CO_2 exposure that does not appear to be a consequence of decreased pH_e, or pH_i, which remained consistent under our experimental conditions **(Fig.S2)**.

RelB is cleaved at its C-terminal in response to elevated CO_2.

We next developed an overexpression system to test RelB sensitivity in HEK cells. The purpose of this was to allow us to perform mass spectrometric interactome studies in cells exposed to elevated CO_2, looking at RelB and its associated proteins (e.g. p100/p52). HEK cells that had been transfected with a full-length N-terminal FLAG-tagged RelB construct **(Fig. 2A)**, re-capitulated the previously observed RelB response to elevated CO_2 **(Fig. 1A & D, Fig S1A-C)** (12). Interestingly, the banding pattern for RelB and FLAG from the HEK cells was almost identical **(Fig.2B & C)** suggesting that RelB is cleaved at its C-terminus. Thus, we observed CO_2-dependent regulation of endogenous NF-κB family members p100 and RelB and also re-capitulated CO_2-dependent cleavage of re-combinant RelB. Our next experiments were performed in order to gain insight into the mechanisms governing RelB sensitivity to CO_2 as well as the consequences for RelB protein-protein interactions.

The RelB interactome is altered by CO_2 exposure.

RelB expression and cellular localisation is altered in response to CO_2 (**Fig1A & D, Fig 2B &C and Fig S1A-C.)** (12). Thus, we hypothesised that these changes were being driven at least in part by altered RelB-protein-protein interactions in the different CO_2 environments. We tested this hypothesis in an unbiased and quantitative manner. We first overexpressed FLAG-RelB in HEK cells, exposed the cells to ambient or elevated CO_2 under pH buffered conditions and performed an immunoprecipitation for FLAG. Precipitated proteins were then analysed by mass spectrometry (**Fig.3A)**. Proteins of interest were then determined by meeting specific stringency thresholds for (i) enrichment over control (non FLAG-RelB expressing cells) and (ii) evidence for CO_2 sensitivity in the RelB-specific protein interactions (2- fold difference up or down) (**Fig 3B)**. Several known RelB- interacting proteins were identified by the screen, which supports the sensitivity of our experimental approach (**Fig 3C)**. E.g. IκBα, importin alpha-7 and ubiquitin carboxyl-terminal hydrolase -7 (the most enriched, 50th most enriched and 90th most enriched interaction respectively) (www.ebi.ac.uk/intact). Regarding CO_2 sensitivity, 25 proteins met or exceeded the thresholds for being a FLAG-RelB associated protein that were differentially associated with RelB in a CO_2-dependent manner. These proteins are listed in (**Fig. S3).** With a selection of proteins illustrated in **(Fig. 4).** 7 proteins demonstrated increased association with FLAG-RelB and 18 proteins demonstrated decreased association with FLAG-RelB at 10% CO_2 compared to ambient CO_2. Interestingly, when Gene

ontology analysis was performed on the 25 proteins that were found to have differential interactions with RelB in a CO_2-dependent manner, there was a strong enrichment of proteins involved in both protein transport and nucleic acid binding **(Fig. S4)**. These unbiased data support the concept that RelB translocates to the nucleus in a CO_2 dependent manner, conceivably facilitated by importin proteins. Selected proteins were chosen for validation of the MS/MS screen by FLAG-RelB overexpression coupled to conventional western blot. RelB interactions with p100 were not affected by CO_2 exposure (**Fig.S5A)**. IκBα had reduced association with RelB at 10% CO_2 in several experiments (**Fig.S5**, while Raf-1 had increased association at 10% CO_2 (**Fig.S5C)**. Thus, the data from these IP western blot experiments supports the IP MS/MS data. Of note, SMARCD2 was markedly enriched with FLAG-IP, but was not consistently different in 10% CO_2 by IP western (**Fig. S5D)**. Thus, the IP western data largely validates the mass spectrometry data, with the MS/MS approach likely more sensitive than IP western approaches. However, given the SMARCD2 data we suggest caution in interpreting the data from the more lowly enriched proteins due to a risk of false positives. CO_2 -dependent changes were more reproducibly validated by western blot for highly enriched interactors (e.g. IκBα p100 and Raf-1).

Amino acids 484-503 are involved in CO_2-dependent processing of RelB.

Having identified the CO_2-dependent nuclear translocation and processing of RelB **Fig. 1** we next sought to identify the region of RelB that was being cleaved. Firstly, data from (**Fig. 2B & C)** suggested that RelB was being cleaved in its C-terminal region downstream of S424 (the RelB antibody epitope). Secondly the lower molecular weight form of RelB observed in 10% CO_2 revealed a relatively small (≈10-15 kDa) increase in electrophoretic mobility. Thus, we performed sequential mutagenesis of the C-terminal region of RelB spanning from before (S404) the RelB antibody epitope (as a control) to beyond where we thought the cleavage site to be likely (V524) based on molecular weight. The region downstream of V524 has a predicted molecular weight of <6kDa (www.expasy.org) which was deemed too small to be our region of interest. Thus, to test our hypothesis and gain molecular insight into the effects of CO_2 on RelB, we generated six mutants which individually deleted 20 amino acid segments of human RelB spanning from amino acids 404-524 **Fig 5A**. These mutants were screened for CO_2 sensitivity alongside a full length RelB control. As expected Δ404-423 (which is N-terminal to the S424 RelB antibody epitope and therefore serves as an internal control) demonstrated CO_2 sensitivity analogous to that of wild-type RelB. Furthermore, this CO_2-sensitivity of Δ404-423 was blocked by pre-treatment with the proteasome inhibitor (as observed for wild-type RelB). Similarly, deletions in the regions 424-443, 444-463 and 464-483 demonstrated the same CO_2-sensitivity and MG-132 sensitivity as the wild-type FLAG-RelB construct. Interestingly, the Δ484-503 mutant did not demonstrate CO_2-dependent cleavage, while CO_2 and MG-132 sensitivity was restored in the downstream Δ504-524 mutant (**Fig. 5B)**. Interestingly, these 20 amino acids (LLDDGFAYDPTAPTLFTMLD) reside within a highly conserved region of the protein. Taken together, these data suggest that amino acids 484-503 are within the cleavage site of RelB and/or are involved in transducing the CO_2-dependent cleavage of RelB.

RelB Δ484-579 has altered NF-κB-dependent transcriptional activity. Having identified that absence of amino acids 484-503 rendered RelB insensitive to CO_2- dependent cleavage we hypothesised that under conditions of elevated CO_2 there is an enriched population of C-terminally truncated RelB in the nucleus. We further hypothesised that the truncated form of RelB has altered transcriptional activity and contributes to CO_2 –dependent alterations in gene expression. To test the hypothesis that a truncated form of RelB has altered signaling capabilities we generated a C-terminally truncated form of FLAG- RelB (RelB Δ484-579 also known as

RelBshort) **Fig 6A.** and compared it with wild-type Flag-RelB in an NF-κB - Luciferase assay. TNFα- significantly increased NF-κB-Luciferase activity at 0.1ng/ml and 1ng/ml. Overexpression of RelBshort led to reduced TNFα-stimulated NF-κB -luciferase activity compared to wild-type RelB indicating altered transcriptional activity (**Fig. 6B**). Thus, overexpression of a truncated form of RelB (that mimics the form of RelB that is enriched in the nucleus at 10% CO_2) alters cytokine stimulated NF-κB -dependent transcriptional activity.

Loss of p100 impairs the CO_2-dependent nuclear localisation of RelB.

In order to investigate the mechanisms underpinning CO_2-dependent nuclear localisation of RelB further, we focused on the interaction between p100 and RelB. p100 and RelB regulate each other's stability (42). Furthermore, p100 is known to have an inhibitory role on NF-κB signaling (38) and play a key role in the inhibitory 'kappaBsome'(39,40). Our earlier data demonstrated that despite a marked nuclear accumulation of RelB in response to CO_2, the interaction with p100 remained relatively constant **(Fig. 3C, 4 and S5A)**. This suggested that p100 might also become nuclear localized in response to elevated CO_2 and contribute to the CO_2 dependent effect on NF-κB signaling. Indeed we observed clear p100 nuclear localisation in response to elevated CO_2 (**Fig. 1A & E, Fig. S1A & D)**. These data suggest the possibility of RelB and p100 translocating to the nucleus together as part of a complex. Given the role of p100 in RelB stability (42), we hypothesised that p100 might be required to confer CO_2 sensitivity on RelB. To test this hypothesis we compared the pattern of CO_2-dependent RelB nuclear localisation in wild-type MEF, and in MEF deficient in 'canonical' p105 (*NFKB1*) as well as 'non-canonical' p100 (*NFKB2*). Interestingly, the p100-/- MEF demonstrated an aberrant pattern of nuclear RelB, compared to both the wild-type and p105-/- MEF. In p100-/- MEF the full-length form of RelB was not enriched in the nucleus in response to elevated CO_2, however the lower molecular weight form of RelB was observed (**Fig. 7B, D & F**). Taken together, this suggests that p100 NF-κB is sensitive to CO_2 and that it is required for the normal distribution of RelB in the nucleus under conditions of elevated CO_2.

DISCUSSION

Alterations in CO_2 levels are increasingly being associated with human pathologies e.g COPD where either hypo or hypercapnia increases the hazard ratio for death (3). This observation is supported by *in-vivo* experimentation illustrating the deleterious consequences of elevated CO_2 in the context of infection (6) and in a clinical trial where reducing hypercapnia in COPD patients was beneficial (43). Against this background it is perhaps counterintuitive that therapeutic hypercapnia is being investigated in the context of single lung ventilation (44). There is however emerging evidence for elevated CO_2 being associated in a better outcome in models of inflammation (19), ventilator induced lung injury (45,46), skin graft survival (47) and stretch induced epithelial injury (48). The mechanisms reconciling these seemingly opposing outcomes in hypercapnia are not fully elucidated and are a basis for this study.

Studies in both model organisms as well as human cells and tissues have implicated a role for altered NF-κB -dependent signaling in response to different CO_2 concentrations (9,11,12,14,15,46,49,50). Members of the 'non-canonical' or 'alternative' NF-κB family (IKKα and RelB) have been reported to be CO_2 –sensitive (11,12), as have genes downstream of the Drosophila orthologue *Relish* in flies (9). Thus, we focused our attention on the transcriptionally active component of the non-canonical NF-κB pathway to gain insight into CO_2 sensing and how CO_2 affects NF-κB signaling.

Our data suggest a significant re-arrangement of RelB and p100 within the cell under conditions of elevated CO_2. Mass spectrometry analysis of immunoprecipitated RelB reveals 135 proteins that are 3 fold enriched compared to control. Of these,

several *bone fide* interactors (p100, IκBα and Raf-1) were found to be significantly enriched by mass spectrometry and separately validated by conventional immunoprecipitation coupled to western blot. Approximately 19% of these proteins were differentially associated with RelB in a CO_2-dependent manner. Thus, most Rel-interactions were not-significantly changed by CO_2. This is an interesting observation given that we can clearly observe marked nuclear translocation of RelB in response to elevated CO_2. This suggests that a sub-population of RelB is actually moving into the nucleus in response to CO_2 and/ or that when RelB moves into the nucleus, it does so as a complex with a number of other proteins including e.g. p100. This proposed scenario might also explain why the ratio of RelB: p100 is unchanged by CO_2. What is clear from the mass spectrometry experiment is that there is a difference in the degree of RelB interaction with proteins associated with the nucleus re. nuclear shuttling (importins), nuclear pore (NUP) and DNA binding e.g. (SMARCD2 and RB1) upon exposure to CO_2. RelB has previously been shown to have a physical association with members of the KPNA family (51). Our observed decrease in association between RelB and alpha importin proteins suggests the possibility that RelB is associated with the importin alpha complex in advance of a stimulus, and following CO_2 exposure this interaction is reduced, as a sub-population of RelB translocates to the nucleus. Taken together, these data point to a selective re-arrangement of RelB with its interacting partners in response to CO_2, that facilitates localisation to the nucleus and may interfere with existing RelB-DNA binding complexes.

RelB is subject to multiple post-translational modifications as well as cleavage by a variety of enzymes (33,52,53). Our data indicates that RelB is cleaved at its C-terminal **(Fig. 2B & C)**. Scanning mutagenesis was employed to determine the precise site involved, in order to gain insight into how CO_2 modulates NF-κB-dependent signaling. Here we report that a Δ484-503 deletion mutant of RelB demonstrates aberrant CO_2-dependent processing (**Fig. 5B**). The 484-503 region is C-terminal to the RelB nuclear localisation motif, which explains why both full length and truncated forms of RelB can accumulate in the nucleus in a CO_2-dependent manner. Furthermore, this site is distinct from other sites that have previously been reported to control RelB processing e.g. Asp205 (54), Thr84/Ser552 (53) and Arg85 (52). Thus, we propose that this 20 amino acid **CO_2-R**esponsive **D**omain (CORD) of RelB is involved in CO_2-dependent cleavage of RelB. The crystal structure for this region of the RelB protein has not yet been solved, and *in silico* structural predictions of this region are of low confidence. However, this region 484-503 does lie within the C-terminal transactivation domain of RelB (55). This suggests that RelB proteins deficient in the region C-terminal to the cleavage site may have impaired transcriptional activity. Previous studies have demonstrated the requirement of both N- and C -terminal regions of RelB in the presence of p50- NF-κB for full transactivation (56).

Thus, our data suggests that under conditions of elevated CO_2 RelB is cleaved and that both full length and truncated forms of RelB can then translocate to the nucleus. It is unlikely that both of these forms of RelB have identical transcriptional activity and consequently we generated a RelBshort construct to test this. This truncated form of RelB (which mimics a form of RelB generated in hypercapnia) has impaired NF-κB -dependent transcriptional activity compared to full length RelB **(Fig. 6B)**.

Finally, given the known reciprocal role of p100 in stabilising RelB, we demonstrated for the first time a profound nuclear localisation of p100 in response to elevated CO_2 **(Fig. 1, Fig. 7A, C and Fig. S1A & D)**. This is consistent with our mass spectrometry data indicating that the ratio of RelB:p100 is unchanged at 10% CO_2, and that the two proteins may translocate to the nucleus as a complex. Thus, using MEF deficient in p100, we investigated the requirement of p100 on the RelB response to elevated CO_2. Interestingly, loss of p100 significantly altered the CO_2-dependent nuclear localisation profile of RelB in the nucleus **(Fig. 7B & D)**. Notably, a lower molecular weight form of RelB was

still evident in the nucleus in response to CO_2 in p100-/- MEF. However, the full- length form of RelB that normally accumulates under those conditions did not **(Fig. 7B & F)**. Together, this suggests that p100 is important in the regulation of the RelB response to elevated CO_2 but is dispensable for the cleavage. Thus, nuclear p100 localisation appears to be a key event in co-ordinating the NF-κB-dependent response to elevated CO_2. Interestingly, while we observed both p100 and p52 translocation to the nucleus in response to CO_2, they did not accumulate to the same extent, with p100 relatively more enriched in the nucleus at 10% CO_2 compared to p52 **(Fig. 7G and Fig. S1F)**. This observation firstly suggests that elevated CO_2 is not driving 'non-canoncial' processing of p100 to p52 and secondly that a repressive p100 and RelB containing complex is enriched in response to CO_2.

In summary hypercapnia is feature of a number of pathologies and is known to modulate innate and immune signaling. A role for the NF-κB pathway downstream of hypercapnia has been proposed however, the mechanisms are not fully elucidated. Targeting CO_2 dependent signaling may represent a new anti-inflammatory strategy in the treatment of human disease however, the molecular mechanisms downstream of CO_2 need to be more fully described. Recently, RelB has been proposed as a potential novel marker of health outcomes in exacerbated COPD (57), a condition linked to hypercapnia. Here we show that RelB is a CO_2 sensitive transcription factor that undergoes a complex cellular re-arrangement under conditions of elevated CO_2. RelB demonstrates decreased association with importin proteins, CO_2-dependent cleavage at its C-terminal that requires AAs 484-503, and translocates to the nucleus both as a full length protein and as a cleaved short form. RelBshort (a truncated form of RelB) demonstrates decreased NF-κB -dependent transcriptional activity compared to wild-type, which may be due to impairment of its transactivation domain and consequent ability to bind nuclear proteins. The RelB interactome is altered in response to CO_2 but several RelB-protein interactions are maintained at 10% CO_2 e.g. interactions with p100. p100, like RelB also translocates to the nucleus under conditions of elevated CO_2 and loss of p100 impairs RelB nuclear localisation when CO_2 levels are elevated. Interestingly, in a recent cohort study of patients requiring acute mechanical ventilation, $PaCO_2$ was an independent predictor of survival to hospital discharge over a linear range of $PaCO_2$ pressures from hypocapnia (<35mmHg) to hypercapnia (66-75mmHg) (58). Thus, a better understanding of the molecular mechanisms underpinning CO_2-dependent NF-κB regulation will enhance our understanding of human pathologies where hypercapnia is a feature and help to develop CO_2 -dependent therapeutic strategies.

MATERIALS AND METHODS

Cell Culture and Exposure to different CO_2 environments— Human embryonic kidney (HEK), mouse embryonic fibroblast (MEF) cells and A549 cells were cultured at ambient O_2 and 5% CO_2 and maintained in a humidified tissue culture incubator prior to exposure to the conditions indicated in the individual experiments.

Temperature was maintained at 37 °C in a humidified environment. CO_2 incubation was achieved by exposure of cells to preconditioned medium in an environmental chamber (COY laboratories (MI USA)) set at 5% or 10% CO_2 with a balance of air. Ambient CO_2 experiments were carried out in a 37 °C humidified incubator with room air.

For experiments involving exposure to 0.03%, 5% and 10% CO_2, pH buffering was achieved by supplementing high glucose DMEM powder (D1152 Sigma) with different amounts of $NaHCO_3$ as described previously (12). Media was then reconstituted, filter-sterilized and supplemented with FCS (10%) and penicillin/streptomycin. NaCl was supplemented to correct for osmolality differences. Taken together this approach can maintain pH_e over a range of CO_2 concentrations (0.03%-10%)

Western Blot Analysis: Nuclear, cytosolic, whole cell, or immunoprecipitated lysates were separated by SDS-PAGE, transferred to

nitrocellulose membranes, and immunoblotted as described previously (11). Primary antibodies against RelB (# 4954) (Fig. 1, 6 & 7) and (#4922) (Fig. S1), p100 (#4882) and lamin (#4777) (Cell Signaling Technology); α-Tubulin (sc-8035) (Santa Cruz Biotechnology); FLAG (#F7425) and β-actin (#A5316) (Sigma-Aldrich) were used, as well as species-specific HRP-conjugated secondary antibodies.

Molecular cloning/mutagenesis: hFLAG-RelB in a pCR3 (Invitrogen) backbone underwent site-directed mutagenesis of its C-terminal region using QuikChange XL-mutagenesis kit according to the manufacturer's instructions. The QuikChange primer design tool was used to generate a series of deletion mutants using the following specific primers.

- **A mutant Δ404-423 F:**
5'-ctcgcgaccatgacagctctgaccccca-3'

Δ404-423 R:
5'-tgggggtcagagctgtcatggtcgcgag-3'

- **B mutant Δ424-443 F:**
5'-cttggggagctgaaccacttcctgcccaac-3'

Δ424-443 R:
5'-gttgggcaggaagtggttcagctccccaag-3'

- **C mutant Δ444-463 F:**
5'-ccggccatcctggaccctgacttcttctct-3'

Δ 444-463 R:
5'-agagaagaagtcagggtccaggatggccgg-3'

- **D mutant Δ 464-483 F:**
5'-ccctgctgccagacctcctggacgatgg-3'

Δ 464-483 R:
5'-ccatcgtccaggaggtctggcagcaggg-3'

- **E mutant Δ 484-503 F:**
5'-gcgggcctgacctgctgccccc-3'

Δ 484-503 R:
5'-gggggcagcaggtcaggcccgc-3'

- **F mutant Δ 504-523 F:**
5'-ttcaccatgctggacgtggttggggagacc-3'

Δ 504-523 R:
5'-ggtctccccaaccacgtccagcatggtgaa-3'

- **RelBshort Δ 484-579 F:**
5'-ccctggcgggcctgactagaagcttgaattctg-3'

Δ 484-579 R:
5'-cagaattcaagcttctagtcaggcccgccaggg-3'

Mutations were confirmed by sequencing using forward T7 and /or pCR3.1-BGHrev primers.

Transfection. Cells were transfected using plasmid DNA, Optimem1 serum free media (Gibco) and Lipofectamine 2000 (Invitrogen) according to the manufacturer's instructions in antibiotic free media. Plasmids for RelB and RelB mutants are described above.

Immunoprecipitation: HEK cells overexpressing recombinant FLAG-tagged proteins were lysed in whole cell lysis buffer (1% Triton X-100, 20mM Tris-HCl (pH7.5), 150mM NaCl, 1mM $MgCl_2$) and incubated with anti-FLAG M2 affinity gel (7.5-15µl/ eppendorf) end over end with rotation at 4 °C for 1-2hrs. Samples were centrifuged at 500 rpm for 1 minute to pellet the beads, which were then washed x 2 in lysis buffer and x 2 in wash buffer (lysis buffer w/o Triton X-100) with centrifugation in between each wash step. Beads were then incubated with NuPAGE sample buffer (≈30-60µl) and boiled for 5 mins. The supernatant was collected, supplemented with 100mM DTT and boiled for a further 5 mins. Samples were then frozen at -20°C or immediately run on a western blot.

Mass spectrometry: Following immunoprecipitation, samples were treated as followed for MS analysis. After washing twice with 300µL ice cold PBS, beads with bound proteins were eluted in two steps. First, by using 60 µL of eluting buffer I (50 mM Tris·HCl(pH 7.5), 2 M urea and 50 µg/mL trypsin (modified sequencing grade trypsin); Promega) and incubated while shaking at

27 °C for 30 min, and second, by adding twice 25 µL of elution buffer II (50 mM Tris·HCl (pH 7.5), 2 M urea and 1 mM DTT). Both supernatants were combined and incubated overnight at room temperature. Samples were alkylated (20 µL iodoacetamide, 5 mg/mL, 30 min in the dark). Then, the reaction was stopped with 1 µL 100% trifluoracetic acid (TFA) and 100 µL of the sample was immediately loaded into equilibrated hand-made
C18 StageTips containing Octadecyl C18 disks (Supelco). Samples were desalted by using two times 50 µL of 0.1% TFA and eluted with two times 25 µL of 50% AcN and 0.1% TFA solution. Final eluates were combined and concentrated until volume was reduced to 5 µL, using a CentriVap concentrator (Labconco). Samples were diluted to obtain a final volume of 12 µL by adding 0.1% TFA. The samples were run on a Q-Exactive mass spectrometer (Thermo Scientific) connected to a Dionex Ultimate 3000 (RSLCnano) chromatography system (ThermoScientific). Each sample was loaded onto Biobasic Picotip Emitter (120 mm length, 75 µm internal diameter) packed with Reprocil Pur C18 (1.9 µm) reverse phase media column and was separated by an increasing acetonitrile gradient, using a 53-min reverse phase gradient at a flow rate of 250 nL/min. The mass spectrometer was operated in positive ion mode with a capillary temperature of 220 °C and a capillary voltage of 1,900 V applied to the capillary. All data were acquired with the mass spectrometer operating in automatic data-dependent switching mode. A high-resolution MS scan (350–2,000 Da) was performed using the Orbitrap to select the 12 most intense ions before MS/MS analysis using the Ion trap. Raw files were analyzed and relative protein concentration and identifications were determined by label-free quantification using the MaxQuant software suite (9). MS/MS spectra were searched against the human UniProt database. Triplicate biological samples for each treatment were performed in each case. Each individual biological sample was then run in duplicate on the mass spectrometer. Each of the triplicate biological samples was considered as an individual n-number for the purposes of this experiment and to determine statistical significance. We have used a similar approach previously (59).

Filtering of Mass Spectrometry Mass Spectrometry Data:
Protein mass spectrometry label-free quantification (LFQ) intensity values were normalized in each replicate for the respective experimental treatments. In order to discriminate specific FLAG-RelB associated interactions, from non-specific FLAG-agarose interactions we defined several inclusion criteria.
(i) Enriched interactions
Proteins that were enriched >3fold in the 0.03% CO_2 and 10% CO_2 FLAG-RelB sample compared to their respective pcDNA- control sample at 0.03% and 10% CO_2 with a p-value of </= 0.05 in each case. 135 proteins were enriched with FLAG-RelB using this analysis
(ii) CO_2 -sensitive interactions
Proteins that were enriched as per (i) above were additionally filtered for CO_2 sensitivity (Ratio FLAG-RelB 10% CO_2: FLAG-RelB 0.03% CO_2, >2 or <0.05) (2- fold difference up or down). 25 proteins had a CO_2 sensitive interaction with FLAG-RelB using this analysis.

Pathway analysis of mass spectrometry mass spectrometry data. 25 CO_2 sensitive protein interactions (see (ii) above in Filtering of Mass spec data and Fig. S1) were analysed for protein class using Panther bioinformatic software www.pantherdb.org.

Densitometry: Densitometric analysis was carried out using ImageJ software to determine band size/intensity of target proteins on western blots and normalized to respective controls e.g. α-Tubulin, Lamin A/C or FLAG.

Luciferase assay: HEK cells were seeded on 24 well plates (50k cells/well). 24hrs later cells were co-transfected with NFκB-Luc PEST (Promega) and β-galactosidase control plasmid along with pcDNA or wt h-FLAG-RelB or FLAG-RelBshort mutant RelB. 24 hrs

later cells were treated +/- TNFα (0.1-1ng/ml) (Sigma) for 24hrs prior to lysis. Lysate was incubated with luciferase substrate (Promega) and chemiluminescence was detected on a BIO-TEK Synergy-HT plate reader.

Intracellular pH (pHi) assay:
This experiment was performed as described previously (11). Briefly, cells were washed in Optimem1(Gibco) serum free media and loaded with 5μM BCECF-AM (Molecular Probes Code B1170) in Optimem1 for 30 mins at 37°C, 21% O_2, 5% CO_2. Dye was removed and cells were incubated in full DMEM media for 30 mins at 37°C, 21% O_2, 5% CO_2. Cells were then exposed to pre-equilibrated buffered media at 0.03% CO_2, 5% or 10% CO_2 for 75mins. Following exposure cells were removed and immediately assayed in a fluorescent plate-reader at RT at 21% O_2, ambient CO_2. The fluorophore was excited at 485nm (λ1) and 444nm (λ2) and emission was recorded at 538nm in each case. The ratio λ1:λ2 is directly proportional to intracellular pH which was confirmed using a standard curve of nigericin (Sigma) permeabilised cells exposed to a high potassium buffer (KCl (140mm), $MgCl_2$ (1mM), $CaCl_2$ (2mM), D-glucose (5mM) adjusted to a range of pH values (pH 5-8) using MES (20mM) acidifying solution or Tris base (20mM) alkalysing solution.

ACKNOWLEDGEMENTS
We thank Dr. Margot Thome (University of Lausanne) for the generous gift of hFLAG-RelB, Prof. Alex Hoffmann (University of California Los Angeles) for generously providing the wild-type, RelB-/-, p100-/- and p105-/- MEF. We acknowledge funding from Science Foundation Ireland (15/CDA/3490), University College Dublin School of Medicine and UCD Research (SF1146).

CONFLICT OF INTEREST
The authors declare that they have no conflicts of interest with the contents of this article.

AUTHOR CONTRIBUTIONS
CEK, CCS, JR, ACS, AvonK, EPC designed, performed and analysed experiments. EPC conceived and coordinated the study and wrote the paper. All authors reviewed the results and approved the manuscript.

REFERENCES

1. Cummins, E. P., Selfridge, A. C., Sporn, P. H., Sznajder, J. I., and Taylor, C. T. (2013) Carbon dioxide-sensing in organisms and its implications for human disease. *Cell Mol Life Sci*
2. Crummy, F., Buchan, C., Miller, B., Toghill, J., and Naughton, M. T. (2007) The use of noninvasive mechanical ventilation in COPD with severe hypercapnic acidosis. *Respiratory medicine* **101**, 53-61
3. Ahmadi, Z., Bornefalk-Hermansson, A., Franklin, K. A., Midgren, B., and Ekström, M. P. (2014) Hypo- and hypercapnia predict mortality in oxygen-dependent chronic obstructive pulmonary disease: a population-based prospective study. *Respiratory research* **15**, 30
4. Roberts, B. W., Karagiannis, P., Coletta, M., Kilgannon, J. H., Chansky, M. E., and Trzeciak, S. (2015) Effects of PaCO2 derangements on clinical outcomes after cerebral injury: A systematic review. *Resuscitation* **91**, 32-41
5. Jaitovich, A., Angulo, M., Lecuona, E., Dada, L. A., Welch, L. C., Cheng, Y., Gusarova, G., Ceco, E., Liu, C., Shigemura, M., Barreiro, E., Patterson, C., Nader, G. A., and Sznajder, J. I. (2015) High CO2 levels cause skeletal muscle atrophy via AMPK, FoxO3a and muscle-specific ring finger

protein1 (MuRF1). *The Journal of biological chemistry*

6. Gates, K. L., Howell, H. A., Nair, A., Vohwinkel, C. U., Welch, L. C., Beitel, G. J., Hauser, A. R., Sznajder, J. I., and Sporn, P. H. (2013) Hypercapnia Impairs Lung Neutrophil Function and Increases Mortality in Murine Pseudomonas Pneumonia. *Am J Respir Cell Mol Biol*
7. Cummins, E. P., and Keogh, C. E. (2016) Respiratory gases and the regulation of transcription. *Exp Physiol* **101**, 986-1002
8. Sharabi, K., Hurwitz, A., Simon, A. J., Beitel, G. J., Morimoto, R. I., Rechavi, G., Sznajder, J. I., and Gruenbaum, Y. (2009) Elevated CO2 levels affect development, motility, and fertility and extend life span in Caenorhabditis elegans. *Proc Natl Acad Sci U S A* **106**, 4024-4029
9. Helenius, I. T., Krupinski, T., Turnbull, D. W., Gruenbaum, Y., Silverman, N., Johnson, E. A., Sporn, P. H., Sznajder, J. I., and Beitel, G. J. (2009) Elevated CO2 suppresses specific Drosophila innate immune responses and resistance to bacterial infection. *Proc Natl Acad Sci U S A* **106**, 18710-18715
10. Li, G., Zhou, D., Vicencio, A. G., Ryu, J., Xue, J., Kanaan, A., Gavrialov, O., and Haddad, G. G. (2006) Effect of carbon dioxide on neonatal mouse lung: a genomic approach. *Journal of applied physiology (Bethesda, Md. : 1985)* **101**, 1556-1564
11. Cummins, E. P., Oliver, K. M., Lenihan, C. R., Fitzpatrick, S. F., Bruning, U., Scholz, C. C., Slattery, C., Leonard, M. O., McLoughlin, P., and Taylor, C. T. (2010) NF-kappaB links CO2 sensing to innate immunity and inflammation in mammalian cells. *J Immunol* **185**, 4439-4445
12. Oliver, K. M., Lenihan, C. R., Bruning, U., Cheong, A., Laffey, J. G., McLoughlin, P., Taylor, C. T., and Cummins, E. P. (2012) Hypercapnia induces cleavage and nuclear localization of RelB protein, giving insight into CO2 sensing and signaling. *J Biol Chem* **287**, 14004-14011
13. Taylor, C. T., and Cummins, E. P. (2011) Regulation of gene expression by carbon dioxide. *J Physiol* **589**, 797-803
14. Takeshita, K., Suzuki, Y., Nishio, K., Takeuchi, O., Toda, K., Kudo, H., Miyao, N., Ishii, M., Sato, N., Naoki, K., Aoki, T., Suzuki, K., Hiraoka, R., and Yamaguchi, K. (2003) Hypercapnic acidosis attenuates endotoxin-induced nuclear factor-[kappa]B activation. *Am J Respir Cell Mol Biol* **29**, 124-132
15. O'Toole, D., Hassett, P., Contreras, M., Higgins, B. D., McKeown, S. T., McAuley, D. F., O'Brien, T., and Laffey, J. G. (2009) Hypercapnic acidosis attenuates pulmonary epithelial wound repair by an NF-kappaB dependent mechanism. *Thorax* **64**, 976-982
16. Abolhassani, M., Guais, A., Chaumet-Riffaud, P., Sasco, A. J., and Schwartz, L. (2009) Carbon dioxide inhalation causes pulmonary inflammation. *American journal of physiology. Lung cellular and molecular physiology* **296**, 65
17. Wang, N., Gates, K. L., Trejo, H., Favoreto, S., Schleimer, R. P.,

Sznajder, J. I., Beitel, G. J., and Sporn, P. H. (2010) Elevated CO2 selectively inhibits interleukin-6 and tumor necrosis factor expression and decreases phagocytosis in the macrophage. *FASEB journal : official publication of the Federation of American Societies for Experimental Biology* **24**, 2178-2190

18. O'Croinin, D. F., Nichol, A. D., Hopkins, N., Boylan, J., O'Brien, S., O'Connor, C., Laffey, J. G., and McLoughlin, P. (2008) Sustained hypercapnic acidosis during pulmonary infection increases bacterial load and worsens lung injury. *Crit Care Med* **36**, 2128-2135
19. Laffey, J. G., Honan, D., Hopkins, N., Hyvelin, J. M., Boylan, J. F., and McLoughlin, P. (2004) Hypercapnic acidosis attenuates endotoxin-induced acute lung injury. *Am J Respir Crit Care Med* **169**, 46-56
20. Costello, J., Higgins, B., Contreras, M., Chonghaile, M. N., Hassett, P., O'Toole, D., and Laffey, J. G. (2009) Hypercapnic acidosis attenuates shock and lung injury in early and prolonged systemic sepsis. *Crit Care Med* **37**, 2412-2420
21. Otulakowski, G., and Kavanagh, B. P. (2011) Hypercapnia in acute illness: sometimes good, sometimes not. *Critical care medicine* **39**, 1581-1582
22. Ghosh, S., and Hayden, M. S. (2012) Celebrating 25 years of NF-kappaB research. *Immunol Rev* **246**, 5-13
23. Millet, P., McCall, C., and Yoza, B. (2013) RelB: an outlier in leukocyte biology. *Journal of leukocyte biology* **94**, 941-951
24. Yilmaz, Z. B., Weih, D. S., Sivakumar, V., and Weih, F. (2003) RelB is required for Peyer's patch development: differential regulation of p52-RelB by lymphotoxin and TNF. *The EMBO journal* **22**, 121-130
25. Weih, F., Carrasco, D., Durham, S. K., Barton, D. S., Rizzo, C. A., Ryseck, R. P., Lira, S. A., and Bravo, R. (1995) Multiorgan inflammation and hematopoietic abnormalities in mice with a targeted disruption of RelB, a member of the NF-kappa B/Rel family. *Cell* **80**, 331-340
26. Dobrzanski, P., Ryseck, R. P., and Bravo, R. (1993) Both N-and C-terminal domains of RelB are required for full transactivation: role of the N-terminal leucine zipper-like motif. *Molecular and cellular ...*
27. Moorthy, A. K., Huang, D.-B. B., Wang, V. Y., Vu, D., and Ghosh, G. (2007) X-ray structure of a NF-kappaB p50/RelB/DNA complex reveals assembly of multiple dimers on tandem kappaB sites. *Journal of molecular biology* **373**, 723-734
28. Caamaño, J., Alexander, J., and Craig, L. (1999) The NF-κB family member RelB is required for innate and adaptive immunity to Toxoplasma gondii. *The Journal of ...*
29. Baglole, C. J., Maggirwar, S. B., and Gasiewicz, T. A. (2008) The aryl hydrocarbon receptor attenuates tobacco smoke-induced cyclooxygenase-2 and prostaglandin production in lung fibroblasts through regulation of

the NF-κB …. *Journal of Biological ...*

30. Tando, T., Ishizaka, A., Watanabe, H., Ito, T., Iida, S., Haraguchi, T., Mizutani, T., Izumi, T., Isobe, T., Akiyama, T., Inoue, J.-i., and Iba, H. (2010) Requiem protein links RelB/p52 and the Brm-type SWI/SNF complex in a noncanonical NF-kappaB pathway. *The Journal of biological chemistry* **285**, 21951-21960
31. Bellet, M. M., Zocchi, L., and Sassone-Corsi, P. (2012) The RelB subunit of NFκB acts as a negative regulator of circadian gene expression. *Cell cycle (Georgetown, Tex.)* **11**, 3304-3311
32. Lovas, A., Radke, D., Albrecht, D., Yilmaz, Z. B., Möller, U., Habenicht, A. J., and Weih, F. (2008) Differential RelA- and RelB-dependent gene transcription in LTbetaR-stimulated mouse embryonic fibroblasts. *BMC genomics* **9**, 606
33. Neumann, M., Klar, S., Wilisch-Neumann, A., Hollenbach, E., Kavuri, S., Leverkus, M., Kandolf, R., Brunner-Weinzierl, M. C., and Klingel, K. (2011) Glycogen synthase kinase-3β is a crucial mediator of signal-induced RelB degradation. *Oncogene* **30**, 2485-2492
34. Maier, H. J., Marienfeld, R., Wirth, T., and Baumann, B. (2003) Critical role of RelB serine 368 for dimerization and p100 stabilization. *Journal of Biological ...*
35. Leidner, J., Palkowitsch, L., Marienfeld, U., Fischer, D., and Marienfeld, R. (2008) Identification of lysine residues critical for the transcriptional activity and polyubiquitination of the NF-kappaB family member RelB. *The Biochemical journal* **416**, 117-127
36. Leidner, J., Voogdt, C., Niedenthal, R., Möller, P., Marienfeld, U., and Marienfeld, R. B. (2014) SUMOylation attenuates the transcriptional activity of the NF-κB subunit RelB. *Journal of cellular biochemistry* **115**, 1430-1440
37. Hailfinger, S., Nogai, H., Pelzer, C., Jaworski, M., Cabalzar, K., Charton, J.-E. E., Guzzardi, M., Décaillet, C., Grau, M., Dörken, B., Lenz, P., Lenz, G., and Thome, M. (2011) Malt1-dependent RelB cleavage promotes canonical NF-kappaB activation in lymphocytes and lymphoma cell lines. *Proceedings of the National Academy of Sciences of the United States of America* **108**, 14596-14601
38. Basak, S., Kim, H., Kearns, J. D., Tergaonkar, V., O'Dea, E., Werner, S. L., Benedict, C. A., Ware, C. F., Ghosh, G., Verma, I. M., and Hoffmann, A. (2007) A fourth IkappaB protein within the NF-kappaB signaling module. *Cell* **128**, 369-381
39. Fusco, A. J., Mazumder, A., Wang, V. Y., Tao, Z., Ware, C., and Ghosh, G. (2016) The NF-kappaB subunit RelB controls p100 processing by competing with the kinases NIK and IKK1 for binding to p100. *Science signaling* **9**, ra96
40. Tao, Z., Fusco, A., Huang, D. B., Gupta, K., Young Kim, D., Ware, C. F., Van Duyne, G. D., and Ghosh, G. (2014) p100/IkappaBdelta sequesters and inhibits NF-kappaB through

kappaBsome formation. *Proc Natl Acad Sci U S A* **111**, 15946-15951

41. Labonté L, C. P., Zago M, Bourbeau J, Baglole CJ. (2014) Alterations in the Expression of the NF-κB Family Member RelB as a Novel Marker of Cardiovascular Outcomes during Acute Exacerbations of Chronic Obstructive Pulmonary Disease. *PLoS ONE*
42. Maier, H. J., Marienfeld, R., Wirth, T., and Baumann, B. (2003) Critical role of RelB serine 368 for dimerization and p100 stabilization. *J Biol Chem* **278**, 39242-39250
43. Kohnlein, T., Windisch, W., Kohler, D., Drabik, A., Geiseler, J., Hartl, S., Karg, O., Laier-Groeneveld, G., Nava, S., Schonhofer, B., Schucher, B., Wegscheider, K., Criee, C. P., and Welte, T. (2014) Non-invasive positive pressure ventilation for the treatment of severe stable chronic obstructive pulmonary disease: a prospective, multicentre, randomised, controlled clinical trial. *The Lancet. Respiratory medicine* **2**, 698-705
44. Gao, W., Liu, D. D., Li, D., and Cui, G. X. (2015) Effect of Therapeutic Hypercapnia on Inflammatory Responses to One-lung Ventilation in Lobectomy Patients. *Anesthesiology* **122**, 1235-1252
45. Otulakowski, G., Engelberts, D., Gusarova, G. A., Bhattacharya, J., Post, M., and Kavanagh, B. P. (2014) Hypercapnia attenuates ventilator-induced lung injury via a disintegrin and metalloprotease-17. *J Physiol* **592**, 4507-4521
46. Contreras, M., Ansari, B., Curley, G., Higgins, B. D., Hassett, P., O'Toole, D., and Laffey, J. G. (2012) Hypercapnic acidosis attenuates ventilation-induced lung injury by a nuclear factor-kappaB-dependent mechanism. *Crit Care Med* **40**, 2622-2630
47. Tzeng, Y. S., Wu, S. Y., Peng, Y. J., Cheng, C. P., Tang, S. E., Huang, K. L., and Chu, S. J. (2015) Hypercapnic acidosis prolongs survival of skin allografts. *The Journal of surgical research* **195**, 351-359
48. Horie, S., Ansari, B., Masterson, C., Devaney, J., Scully, M., O'Toole, D., and Laffey, J. G. (2016) Hypercapnic acidosis attenuates pulmonary epithelial stretch-induced injury via inhibition of the canonical NF-kappaB pathway. *Intensive Care Med Exp* **4**, 8
49. Li, A. M., Quan, Y., Guo, Y. P., Li, W. Z., and Cui, X. G. (2010) Effects of therapeutic hypercapnia on inflammation and apoptosis after hepatic ischemia-reperfusion injury in rats. *Chin Med J (Engl)* **123**, 2254-2258
50. Masterson, C., O'Toole, D., Leo, A., McHale, P., Horie, S., Devaney, J., and Laffey, J. G. (2016) Effects and Mechanisms by Which Hypercapnic Acidosis Inhibits Sepsis-Induced Canonical Nuclear Factor-kappaB Signaling in the Lung. *Crit Care Med* **44**, e207-217
51. Bouwmeester, T., Bauch, A., Ruffner, H., Angrand, P.-O. O., Bergamini, G., Croughton, K., Cruciat, C., Eberhard, D., Gagneur, J., Ghidelli, S., Hopf, C., Huhse, B., Mangano, R., Michon, A.-M. M., Schirle, M., Schlegl, J., Schwab, M., Stein, M. A., Bauer, A., Casari, G., Drewes, G., Gavin, A.-C. C., Jackson, D. B., Joberty, G.,

Neubauer, G., Rick, J., Kuster, B., and Superti-Furga, G. (2004) A physical and functional map of the human TNF-alpha/NF-kappa B signal transduction pathway. *Nature cell biology* **6**, 97-105

52. Hailfinger, S., Lenz, G., Ngo, V., Posvitz-Fejfar, A., Rebeaud, F., Guzzardi, M., Penas, E. M., Dierlamm, J., Chan, W. C., Staudt, L. M., and Thome, M. (2009) Essential role of MALT1 protease activity in activated B cell-like diffuse large B-cell lymphoma. *Proc Natl Acad Sci U S A* **106**, 19946-19951
53. Marienfeld, R., Berberich-Siebelt, F., Berberich, I., Denk, A., Serfling, E., and Neumann, M. (2001) Signal-specific and phosphorylation-dependent RelB degradation: a potential mechanism of NF-kappaB control. *Oncogene* **20**, 8142-8147
54. Kuboki, M., Ito, A., Simizu, S., and Umezawa, K. (2015) Activation of apoptosis by caspase-3-dependent specific RelB cleavage in anticancer agent-treated cancer cells: involvement of positive feedback mechanism. *Biochem Biophys Res Commun* **456**, 810-814
55. Perkins, N. D. (2007) Integrating cell-signalling pathways with NF-kappaB and IKK function. *Nat Rev Mol Cell Biol* **8**, 49-62
56. Dobrzanski, P., Ryseck, R. P., and Bravo, R. (1993) Both N- and C-terminal domains of RelB are required for full transactivation: role of the N-terminal leucine zipper-like motif. *Mol Cell Biol* **13**, 1572-1582
57. Labonte, L., Coulombe, P., Zago, M., Bourbeau, J., and Baglole, C. J. (2014) Alterations in the expression of the NF-kappaB family member RelB as a novel marker of cardiovascular outcomes during acute exacerbations of chronic obstructive pulmonary disease. *PLoS One* **9**, e112965
58. Fuller, B. M., Mohr, N. M., Drewry, A. M., Ferguson, I. T., Trzeciak, S., Kollef, M. H., and Roberts, B. W. (2017) Partial pressure of arterial carbon dioxide and survival to hospital discharge among patients requiring acute mechanical ventilation: A cohort study. *J Crit Care* **41**, 29-35
59. Rodriguez, J., Pilkington, R., Garcia Munoz, A., Nguyen, L. K., Rauch, N., Kennedy, S., Monsefi, N., Herrero, A., Taylor, C. T., and von Kriegsheim, A. (2016) Substrate-Trapped Interactors of PHD3 and FIH Cluster in Distinct Signaling Pathways. *Cell Rep* **14**, 2745-2760

FIGURE LEGENDS

Figure 1. Elevated CO_2 causes a cellular re-organisation of the NF-κB family members RelB and p100. (A) MEF were exposed to 0.03, 5% or 10% CO_2 in pH buffered media for 75 mins prior to preparation of cytosolic and nuclear protein fractions. Lysates were immunoblotted using specific antibodies against RelB, p100/p52, Lamin and α-Tubulin. (ns) denotes a non-specific cytosolic band **(B)** Densitometric quantification of cytoplasmic RelB relative to α-Tubulin. **(C)** Denstiometric quantification of cytoplasmic p100 relative to α-Tubulin **(D)** Densitometric quantification of nuclear RelB relative to lamin **(E)** Densitometric quantification of nuclear p100 relative to lamin. Data representative of n=3 experiments.

Figure 2. RelB is cleaved at its C-terminal in reponse to elevated CO_2.

(A) Cartoon indicating the structure of the hFLAG-RelB construct and the region on this protein to which our RelB antibodies are directed (S424). **(B)** HEK cells transiently transfected with hFLAG-RelB were exposed to 0.03% or 10% CO_2 in pH buffered media for 75 mins prior to preparation of nuclear protein fractions. Lysates were immunoblotted using specific antibodies against RelB and **(C.)** FLAG. Data representative of >n=3 experiments.

Figure 3. Mass spectrometric analysis of RelB protein-protein interactions. (A) Cartoon illustrating the experimental workflow leading to the identification of proteins associated with FLAG-RelB. **(B)** Cartoon illustrating the filtering strategy of the LFQ data to identify bone fide RelB interactions, and RelB interactions that are altered by exposure to 10% CO_2. **(C)** Scatter plot of the 135 RelB protein interactions plotted for LFQ FLAG IP intensity (degree of enrichment) versus Ratio LFQ FLAG IP 10% CO_2/ 0.03% CO_2 (CO_2 sensitivity). CO_2 enhanced interactions are shown in red, CO_2 diminished interactions are shown in green, other RelB interactions are shown in blue.

Figure 4. The RelB interactome is altered by CO_2 exposure. HEK cells transiently transfected with pcDNA control plasmid or hFLAG-RelB were exposed to 0.03% or 10% CO_2 in pH buffered media for 75 mins prior to preparation of whole cell lysates. Lysates were immunoprecipitated using FLAG-agarose and precipitated proteins were analysed by mass spectrometry. Data shown are Protein LFQ-intensity values of selected proteins identified in the negative control and the FLAG-RelB IP at 0.03% and 10% CO_2. Selected proteins demonstrating increased association with FLAG-RelB at 10% CO_2 are highlighted in red, selected proteins demonstrating decreased association with FLAG-RelB at 10% CO_2 are highlighted in green.
Data are representative of mean peptide intensity values +/- SD relative to RelB for three biological replicates and two technical replicates per treatment. Statistical analysis comparing FLAG-RelB at 0.03% and 10% CO_2 was performed using a Student's t-test with a p-value </= 0.05 deemed significant. (* p</=0.05, ** p</=0.01, *** p </=.001)

Figure 5. Amino acids 484-503 are involved in CO_2-dependent processing of RelB. (A) HEK cells transiently transfected with full length FLAG-RelB or one of six 20 AA deletions of RelB **(B)** were exposed to 0.03% or 10% CO_2 in pH buffered media for 75 mins +/- Mg-132 (10μM) prior to preparation of nuclear lysates and immunoblotting using a FLAG antibody and Ponceau S staining of the nitrocellulose membrane. Data is representative of > n=3 experiments.

Figure 6. RelB Δ484-579 has altered NF-κB- dependent transcriptional activity. (A) HEK cells were transiently co-transfected with pcDNA control, full length FLAG-RelB (WT) or RelBshort (FLAG-RelB Δ484-579) in addition to a κB-Luciferase promoter reporter construct and a β-galactosidase reporter. **(B)** Cells were treated with TNFα (0, 0.1 & 1ng/ml) for 24hrs at 5% CO_2. Relative light units (RLU) were normalized to β-galactosidase absorbance for each sample. These non-parametric data were normalized by transforming the data by Log10. Data presented is mean +/- SEM for n=4 experiments. Statistical analysis was performed using repeated measures one way ANOVA, with Tukey's multiple comparisons test. A p-value </= 0.05 was deemed significant. (* p</=0.05).

Figure 7. Loss of p100 NF-κB impairs the CO_2-dependent nuclear localisation of RelB. (A), MEF (wild type (wt) *NFkB1*-/- (p105-/-) and *NFkB2-/-* (p100-/-)) were exposed to 0.03% or 10% CO_2 in pH buffered media for 75 mins prior to preparation of nuclear lysates. Lysates were immunoblotted using p100/p52 **(B)** RelB and Lamin specific antibodies **(C)** Densitometric analysis was performed to determine the ratio of p100 **(E)**, p52 and **(D & F)** RelB relative to Lamin. Data shown is mean protein expression +/- SEM relative to control (wt MEF exposed to 0.03% CO_2). **(G)**

Densitometric analysis of the ratio of nuclear p100 relative to nuclear p52 in response to elevated CO_2. Densitometric data is presented as mean +/- SEM for n=4 experiments.

Figure 1.

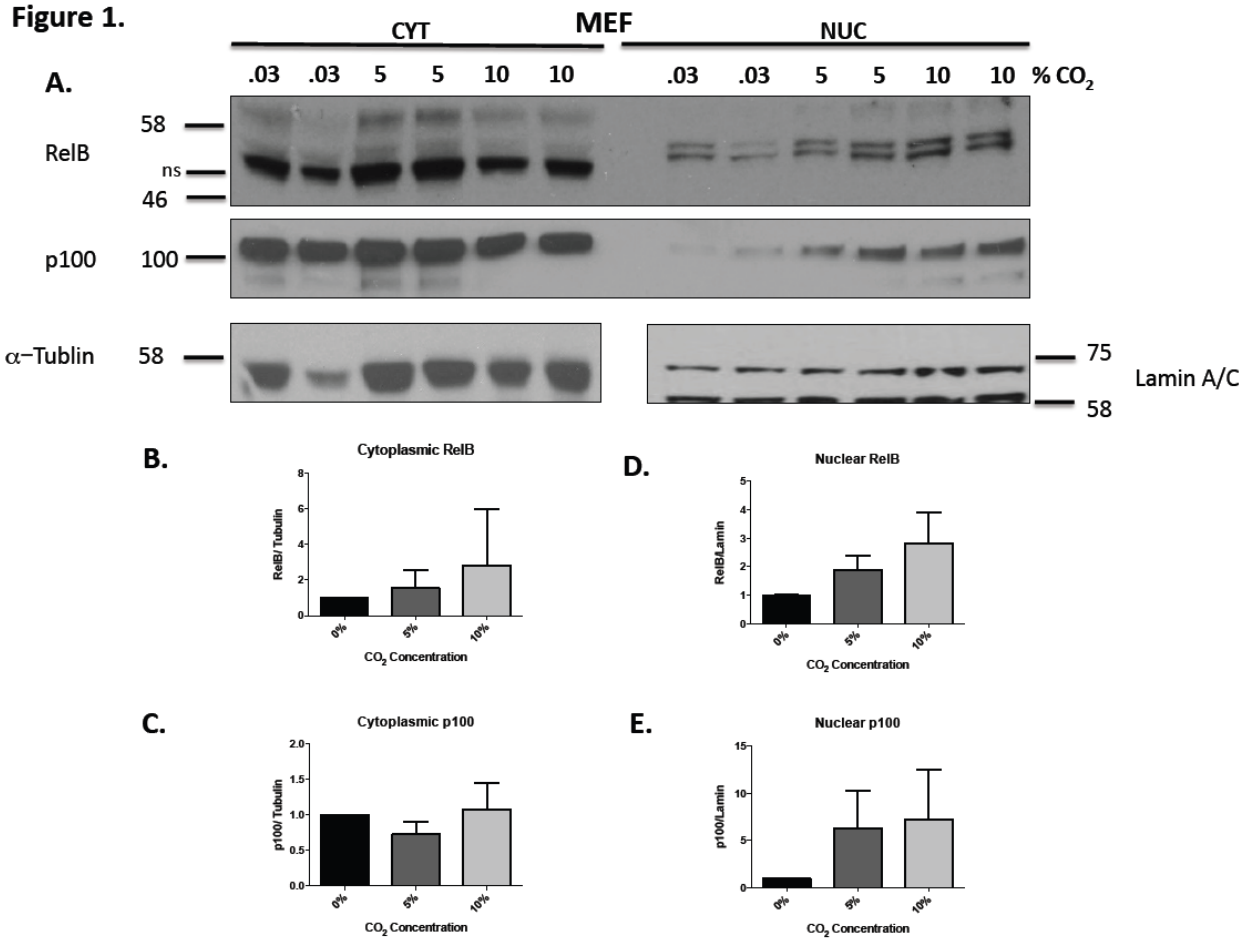
CYT
MEF
NUC
.03 .03 5 5 10 10
.03 .03 5 5 10 10 % CO2
A.
58
RelB
ns
46
p100
100
α–Tublin
58
75
Lamin A/C
58
B.
Cytoplasmic RelB
RelB/ Tubulin
CO2 Concentration
D.
Nuclear RelB
RelB/Lamin
CO2 Concentration
C.
Cytoplasmic p100
p100/ Tubulin
CO2 Concentration
E.
Nuclear p100
p100/Lamin
CO2 Concentration

Figure 2.

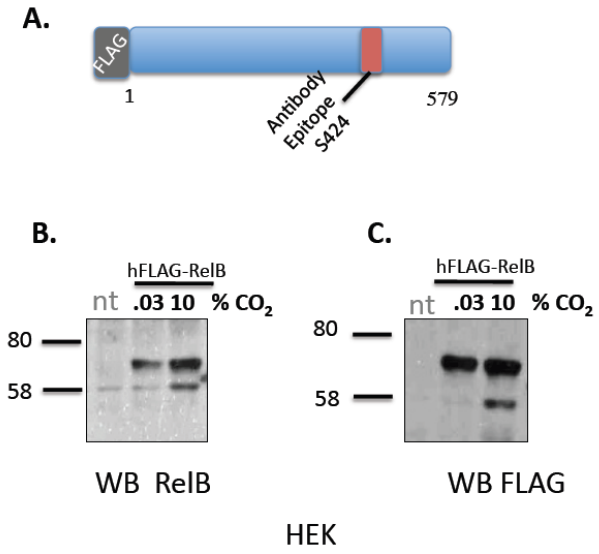
A.
FLAG
1
579
Antibody Epitope S424
B.
hFLAG-RelB
nt .03 10 % CO2
80
58
WB RelB
C.
hFLAG-RelB
nt .03 10 % CO2
80
58
WB FLAG
HEK

Figure 3.

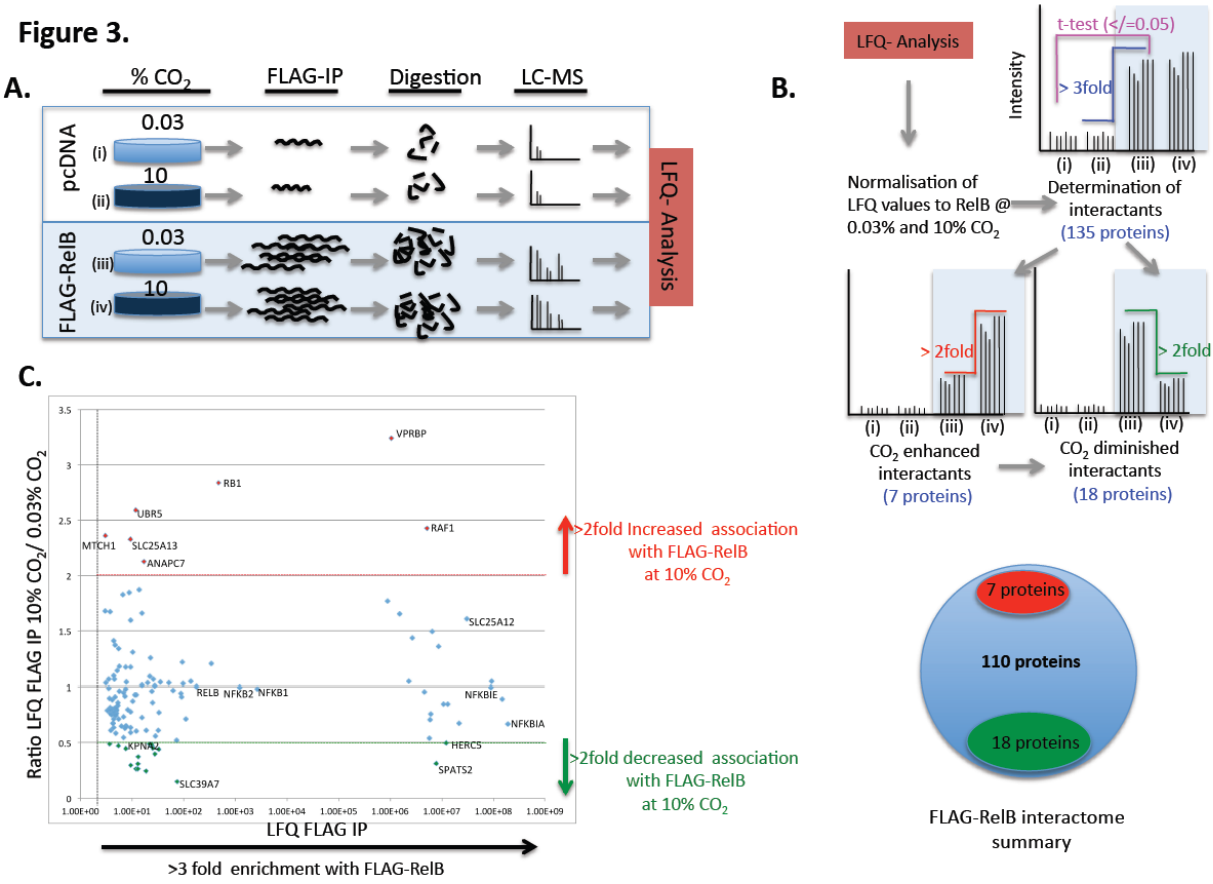
A.
% CO2
FLAG-IP
Digestion
LC-MS
pcDNA
0.03
(i)
10
(ii)
FLAG-RelB
0.03
(iii)
10
(iv)
LFQ- Analysis
B.
LFQ- Analysis
t-test (</=0.05)
> 3fold
Intensity
(i) (ii) (iii) (iv)
Normalisation of LFQ values to RelB @ 0.03% and 10% CO2
Determination of interactants (135 proteins)
> 2fold
> 2fold
(i) (ii) (iii) (iv)
(i) (ii) (iii) (iv)
CO2 enhanced interactants (7 proteins)
CO2 diminished interactants (18 proteins)
7 proteins
110 proteins
18 proteins
FLAG-RelB interactome summary
C.
Ratio LFQ FLAG IP 10% CO2/ 0.03% CO2
LFQ FLAG IP
>3 fold enrichment with FLAG-RelB
VPRBP
RB1
UBR5
RAF1
MTCH1
SLC25A13
ANAPC7
SLC25A12
RELB
NFKB2
NFKB1
NFKBIE
NFKBIA
XPNPEP2
HERC5
SPATS2
SLC39A7
>2fold Increased association with FLAG-RelB at 10% CO2
>2fold decreased association with FLAG-RelB at 10% CO2

Figure 4.

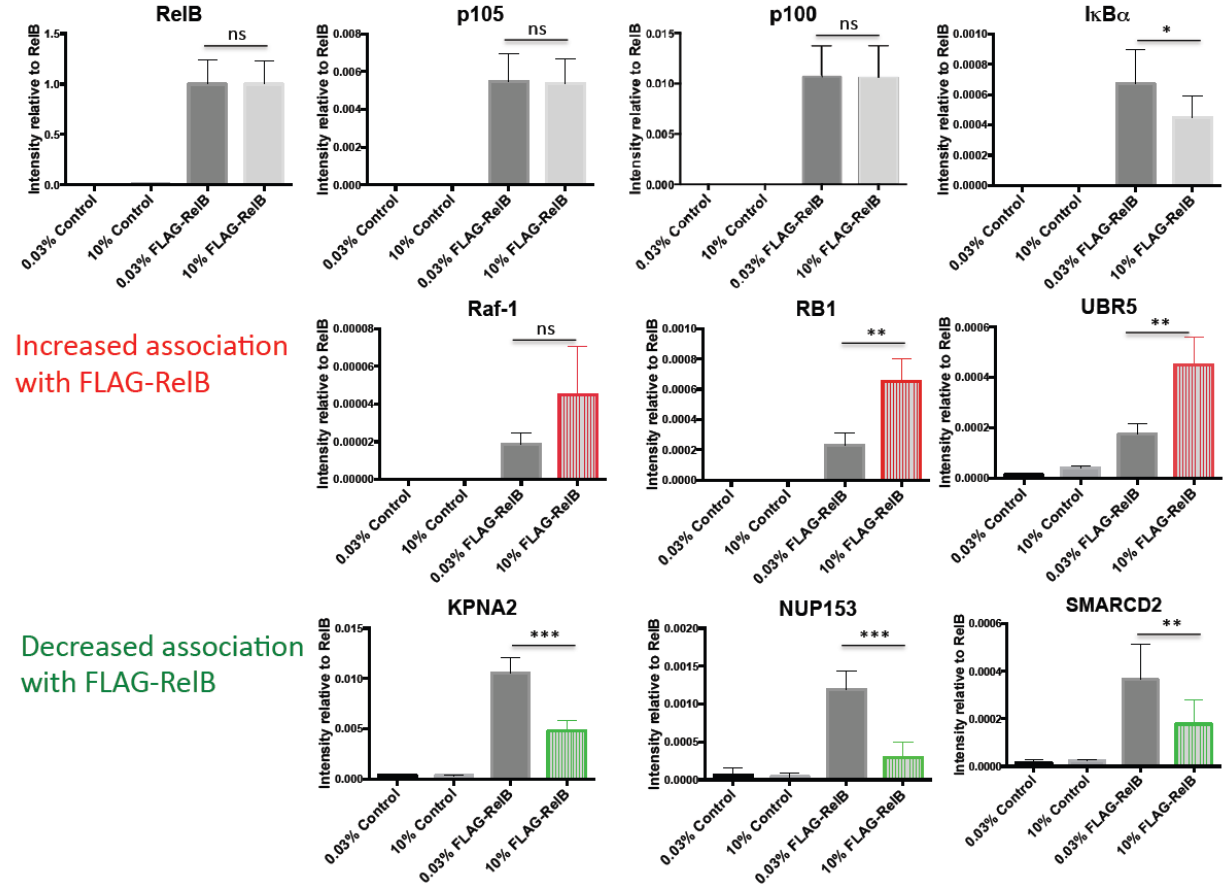
RelB
p105
p100
IκBα
Raf-1
RB1
UBR5
KPNA2
NUP153
SMARCD2
Intensity relative to RelB
ns
*
**
***
0.03% Control
10% Control
0.03% FLAG-RelB
10% FLAG-RelB
Increased association with FLAG-RelB
Decreased association with FLAG-RelB

Figure 5.

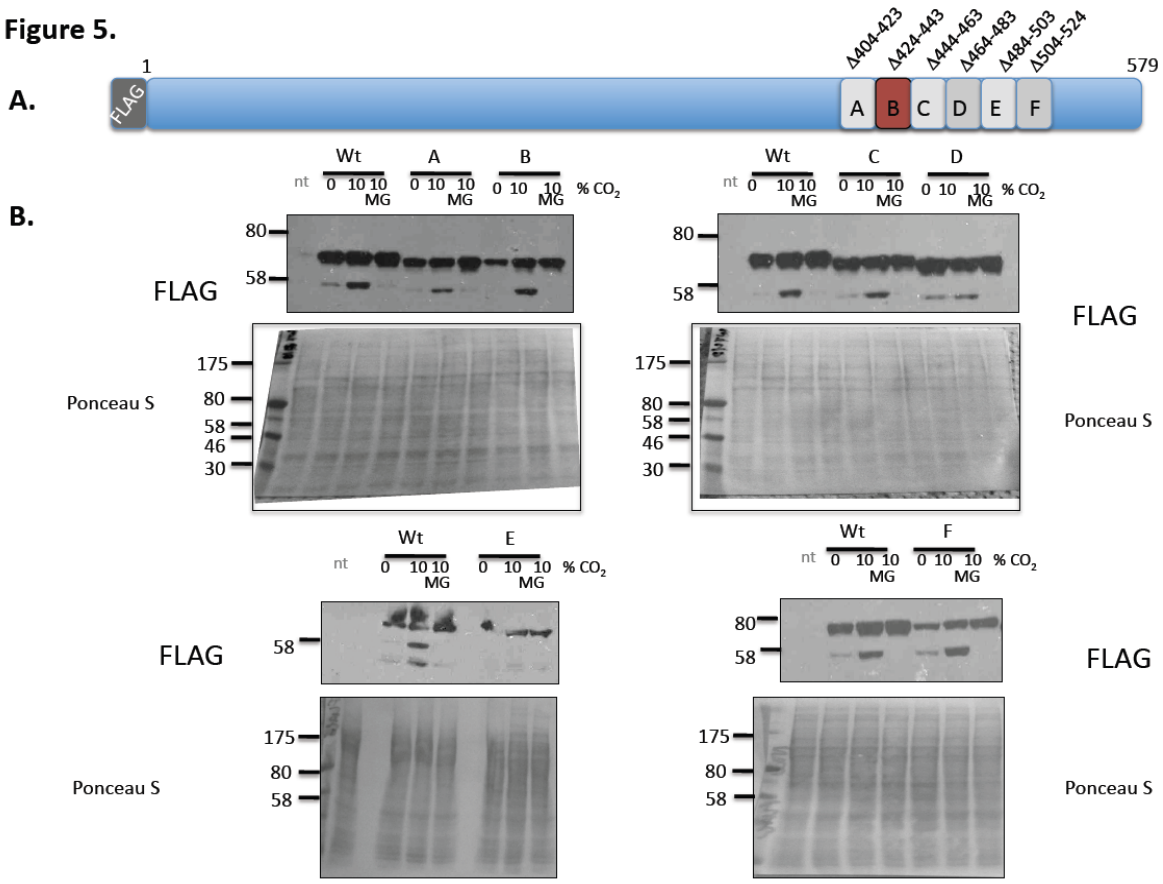
A.
1
579
FLAG
Δ404-423
Δ424-443
Δ444-463
Δ464-483
Δ484-503
Δ504-524
A
B
C
D
E
F
B.
Wt
A
B
C
D
E
F
nt
0 10 10
MG
% CO2
FLAG
Ponceau S
80
58
175
46
30

Figure 6.

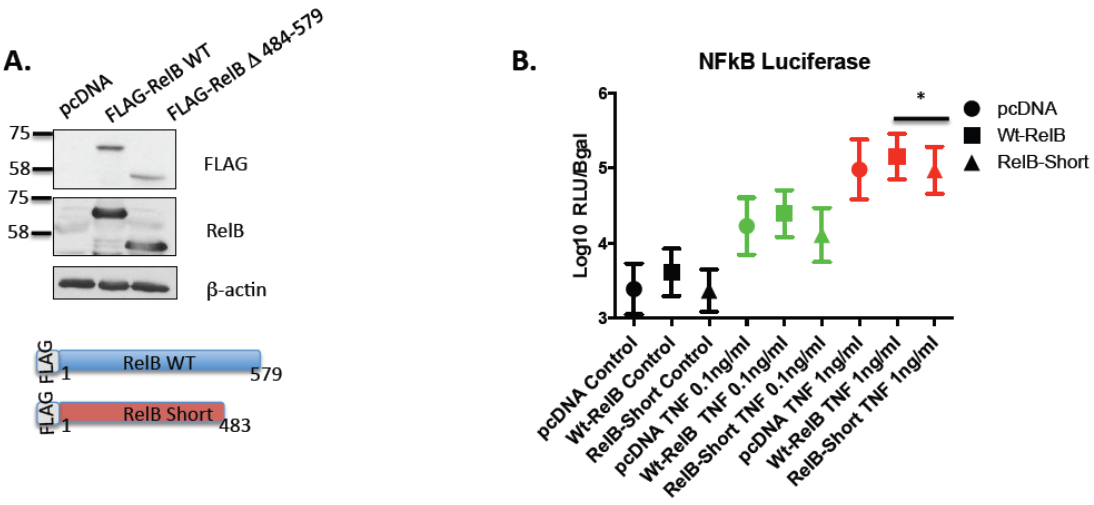
A.
pcDNA
FLAG-RelB WT
FLAG-RelB Δ 484-579
75
58
75
58
FLAG
RelB
β-actin
FLAG
1
RelB WT
579
FLAG
1
RelB Short
483
B.
NFkB Luciferase
Log10 RLU/Bgal
6
5
4
3
*
pcDNA
Wt-RelB
RelB-Short
pcDNA Control
Wt-RelB Control
RelB-Short Control
pcDNA TNF 0.1ng/ml
Wt-RelB TNF 0.1ng/ml
RelB-Short TNF 0.1ng/ml
pcDNA TNF 1ng/ml
Wt-RelB TNF 1ng/ml
RelB-Short TNF 1ng/ml

Figure 7.

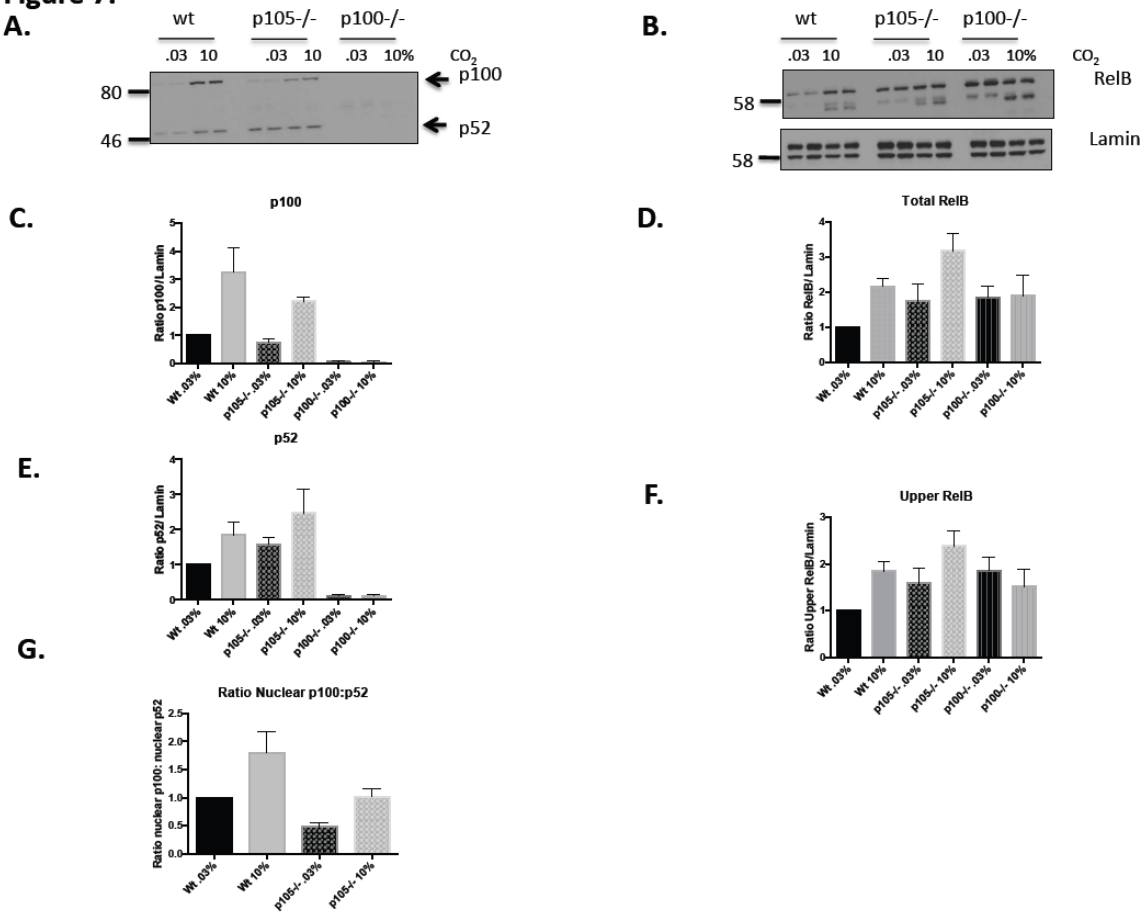
A.
wt
p105-/-
p100-/-
.03 10
.03 10
.03 10%
CO2
80
46
p100
p52
B.
wt
p105-/-
p100-/-
.03 10
.03 10
.03 10%
CO2
58
RelB
58
Lamin
C.
p100
Ratio p100/Lamin
Wt .03%
Wt 10%
p105-/- .03%
p105-/- 10%
p100-/- .03%
p100-/- 10%
D.
Total RelB
Ratio RelB/ Lamin
E.
p52
Ratio p52/ Lamin
F.
Upper RelB
Ratio Upper RelB/Lamin
G.
Ratio Nuclear p100:p52
Ratio nuclear p100: nuclear p52